Transitioning from underdamped to overdamped behavior in theory and in Langevin simulations of desorption of a particle from a Lennard-Jones potential

Alyssa Travitz [a], Ethayaraja Mani [b], and Ronald G. Larson [a, c]

[a] Macromolecular Science and Engineering Program, University of Michigan, Ann Arbor, Michigan 48104, United States

[b] Polymer Engineering and Colloid Science Lab, Department of Chemical Engineering, Indian Institute of Technology Madras, Chennai – 600036, India

[c] Department of Chemical Engineering, University of Michigan, Ann Arbor, Michigan, 48109, United States

Abstract

We investigate the transition between the overdamped and underdamped regimes in Langevin dynamics simulations with significant conservative forces by comparing direct simulations with theory by Kramers, by Mel'nikov and Meshkov, and by Larson and Lightfoot. The need for clarification is made evident by noting that the most commonly cited theories of Kramers and of Mel'nikov and Meshkov (MM) do not apply in the overdamped limit to escape times from a Lennard-Jones (LJ) potential, because Kramers and MM do not account for the flatness of the LJ potential at the escape position, which allows for a region of nearly free Brownian diffusion near the escape position. While the little-known Larson-Lightfoot (LL) approach does consider a Lennard-Jones potential, it does not properly consider the underdamped regime, and so a complete description is only achieved by combining the LL and MM results into a single general equation, which we validate for the first time by explicit comparison with Langevin simulations.

Introduction

Langevin and Brownian dynamics simulations of complex fluids are becoming increasingly common as computational power increases and these tools are being extended to ever more complex systems. While simulations of simple monodisperse polymers and suspensions of spheres have been carried out for many years, such tools can now be applied to more complex systems, including, for example, mixtures of polymers and colloids[1], gelling systems[2], micellar systems[3], semi-flexible polymers, etc.[4] Open-source tools for such simulations are often used instead of homegrown code due to their efficiency, flexibility, and reproducibility. Such open-source

software, including the well-known LAMMPS and HOOMD-blue packages, solve the Langevin equation,[5,6]

$$m_i \frac{d^2 r_i}{dt^2} = -\zeta_i \frac{dr_i}{dt} + F_i^C + F_i^R \qquad \text{Eq. 1}$$

Here, m_i is the mass of i^{th} species, r_i is the particle position, ζ_i is its friction coefficient, F_i^C is the conservative force due to inter- and intra-species interactions, and F_i^R is the random force due to solvent interactions (Gaussian noise). This equation is typically solved at constant NVT (canonical ensemble). In HOOMD-blue, the drag coefficient is directly defined, while in LAMMPS, one specifies the friction coefficient, ζ, via an inertial time defined for each species as

$$t_{in} = \frac{m}{\zeta} \qquad \text{Eq. 2}$$

where the subscript, *i,* denoting the i^{th}species, is omitted here for clarity. Because t_{in} is inversely proportional to the drag coefficient, viscous damping actually becomes weaker as this so-called "damping parameter," as defined in LAMMPS, becomes larger. When $t \ll t_{in}$, a free particle (with $F_i^C = 0$) undergoes ballistic motion dominated by inertia due to its mass m, while for $t \gg t_{in}$, it undergoes diffusive motion dominated by its drag coefficient, ζ. That is, it attains the overdamped *regime* at long times, where inertia becomes unimportant. The limit in which particle mass is taken to be zero is the overdamped *limit*, and solutions of corresponding equations, lacking the acceleration term in Eq. 1, are referred to as "Brownian dynamics," since apart from conservative forces only Brownian forces drive particle motion.

Since most problems of interest in such simulations are concerned with behavior in the overdamped regime, when solving the Langevin equation, one must be careful to choose to achieve the overdamped regime where particle masses no longer affect the results. A simple "rule of thumb" for doing so is to make sure that the inertial time t_{in} is less than any relaxation time relevant to the physical problem, so that inertial effects present at short times have decayed by the time the physics of interest emerge in the solution. While choosing a small value for t_{in} helps ensure

attainment of the overdamped regime, smaller values can be computationally wasteful, since time step sizes generally must be on the order of, or smaller than, t_{in}, unless the mass is set to zero.

Although the above criterion, $t \gg t_{in}$, for attaining the overdamped limit applies to free particle diffusion in the absence of a conservative force, it is well known that when a potential is present, the escape time of the particle from a potential can be affected by inertia even when the particle's escape time is much longer than t_{in}.[7] Much literature addresses this escape time in the presence or absence of inertia, including the classic paper of Kramers,[7] the more recent and complete work of Mel'nikov and Meshkov (MM),[8] and the little-noticed work of Larson and Lightfoot[9] (LL, where this Larson is not an author of our paper). However, we have found that the application of this literature to complex fluid simulations can be confusing, because of several points that need clarifying:

1. When an attractive potential is present, attainment of the overdamped regime is not controlled only by the timescale of the escape relative to the inertial time, $t_{in} = \frac{m}{\zeta}$, but is influenced by the depth and shape of the potential well.
2. The standard Kramers theory, and even the more complete theory by Mel'nikov and Meshkov, only apply to the overdamped regime if the escape from a potential well occurs at a local maximum with downward curvature in the potential. Therefore, these approaches do not apply to conventional and widely used Lennard-Jones potential wells, which become flat at the position where the particle escapes the well.
3. The only theory that considers particle escape from a Lennard-Jones potential is the little-cited work by Larson and Lightfoot. However, their work is also incomplete in its description of the transition to the fully underdamped regime because it does not account for the action of the particle or the entire shape of the potential in limit of small friction.
4. The slope of the potential at the point of escape is irrelevant in the underdamped regime, so that the Mel'nikov-Meshkov (MM) theory correctly describes particle escape in this regime even for a Lennard-Jones potential. As a result, a complete description of particle escape from the LJ potential is obtained by combining the LL theory for the overdamped limit with the MM theory for the underdamped regime.

Because few of those simulating complex fluids seem to be aware all of the above points, as demonstrated by earlier work in our group which includes errors resulting from this ignorance, it is useful to review carefully the implications of the key papers by Mel'nikov and Meshkov (MM), Larson and Lightfoot (LL), and Kramers.[7–10] It is also important to compare the predictions of these theories with Langevin simulations of the escape of a particle from a Lennard-Jones potential well, so that the various regimes and effects of the different approximations are clearly demonstrated and the conditions for transition between underdamped and overdamped regimes are clearly defined. We also seek to provide an expression for the average escape time from a Lennard-Jones potential well that encompasses all regimes of inertia and well depth that can be used in mesoscopic simulations.

Evaluating theoretical approaches

One-dimensional transport of a particle in either free space or in a potential well is described by a Fokker-Planck equation for position and momentum, given in multiple sources.[7,9,11] The non-dimensionalized mean first passage time for particle escape, τ_{esc}/τ_0, is defined as the time for first crossing of a distance criteria, z_{cut} (typically near or at the upper edge of a potential well), where τ_0 is a characteristic frictional time defined as $\tau_0 \equiv \zeta a^2/k_B T$. Assuming a fixed value of z_{cut}, this dimensionless escape time τ_{esc}/τ_0 is a function of two dimensionless groups, namely the dimensionless well depth $\varepsilon/k_B T$ and the dimensionless friction constant $\alpha \equiv \frac{\zeta^2\, a^2}{m\, k_B T}$, where a is the distance unit comparable to the width of the well. The classical and best-known solutions to this problem define the crossing point for escape of the particle to be at the local maximum of the potential well, denoted as z_{cut} in Fig. 1A, providing an unambiguous location for escape beyond which the potential acts as a barrier to re-entry.

The most complete solutions to this problem are those of Kramers and of Mel'nikov and Meshkov, both using a pseudo-steady-state (PSS) approximation, but with Kramers' most "general" solution also assuming that α is "not so small that energy uptake from the heat bath... is a limiting factor in determining the escape rate."[7–9] Kramers handled the limit of "very small" α with a separate asymptotic formula, which was not encompassed by his otherwise "general" solution for damping ranging from moderately damped to overdamped. The Mel'nikov-Meshkov solution, however,

does encompass the case of arbitrarily small α and provides a solution valid for the entire range of α. Both the Kramers and Mel'nikov-Meshkov solutions, however, require the presence of a well-defined potential well $U(x)$ that is sufficiently deep to permit the PSS assumption, with a region of positive curvature defining its bottom, and *a region of negative curvature defining its top*, which is taken as the point z_{cut} beyond which the particle has escaped (see Fig. 1A).

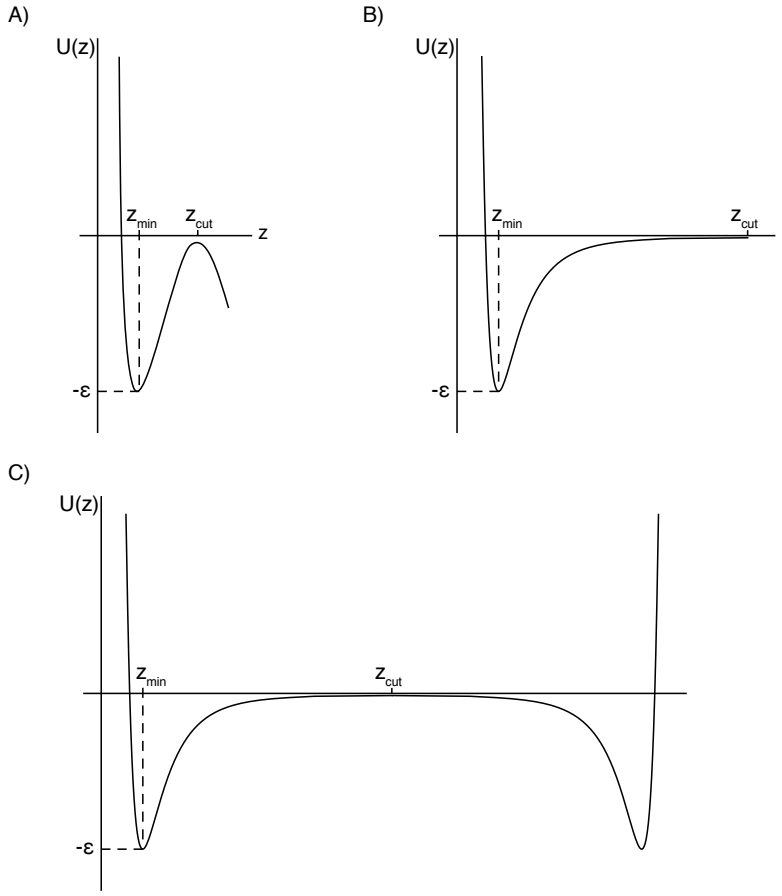

Fig. 1. Schematic of potential curves wherein a Brownian particle is trapped. A) A potential with both a minimum, z_{min}, and a local maximum, z_{cut}. B) A Lennard-Jones potential with a minimum, z_{min}, where z_{cut} is set at some arbitrary position in the flat part of the potential. C) The same as 1B, except superposing a mirror image of the same potential shifted so that z_{cut} of the mirror potential is at the same position as z_{cut} of the original potential.

Thus, both Kramers and Mel'nikov-Meshkov solutions, and in fact, almost the entirety of the literature on this problem, exclude one of the most common potentials, the Lennard-Jones (LJ) potential, which has no local maximum, but only a gradual flattening of the potential at large

distances from its minimum, as shown in Fig. 1B. In this work we consider the 12-6 Lennard-Jones flat wall potential commonly used in HOOMD-blue, LAMMPS, and other simulation packages:

$$U_{LJ}(z) = \begin{cases} 4\varepsilon\left[\left(\frac{\sigma}{z}\right)^{12} - \left(\frac{\sigma}{z}\right)^{6}\right], & z < z_{cut} \\ 0, & z \geq z_{cut} \end{cases} \qquad \text{Eq. 3}$$

Where in our Langevin and Brownian simulations we take $z_{cut} = 2.5\ a,\ \sigma = 1.0\ a,$ and the potential is slightly shifted vertically so that the it smoothly goes to zero at $z_{cut} = 2.5\ a$. We are interested in τ_{esc}, the mean time for a particle to travel from the bottom of the potential well, $z_{min} = 2^{1/6}\ a$ to z_{cut}. All simulations here are performed using the HOOMD-blue Langevin and Brownian integrators in the NVT ensemble.

The one comprehensive paper that explicitly considers the LJ case is that of Larson and Lightfoot (LL), whose solution method is specialized for escape at some arbitrary, relatively large, distance from the local minimum in the LJ potential, which then sets the cut-off value z_{cut} of the potential.[9] While Larson and Lightfoot solved the Fokker-Planck equation for the LJ potential, they did so under the approximation that energy uptake from the heat bath is not limiting, which is not valid for "very small" values of α, as noted above. However, the Kramers and Mel'nikov-Meshkov solutions, while not valid for the LJ potential in the overdamped limit, should become accurate for this potential at small enough α, where only the shape of the potential well around z_{min} is relevant. Therefore, to solve the problem of escape of a particle from an LJ potential in the overdamped limit, the little-known LL solution is necessary, while to solve the escape problem outside of this limit, and to determine the transitions between the different limits, the Kramers and especially the MM solutions are necessary. Our goal is to provide valid solutions for the escape time in each limit for the LJ potential, to define the conditions necessary for each limit to apply, and to provide a cross-over formula that would allow one to bridge between the limits. This includes defining the ranges of α and of ε/k_BT that distinguish between "small" and of "very small" α, where in the latter case the escape time is set by the rate of energy uptake from the heat bath.

1. Overdamped particle

We first consider the overdamped regime, where the diffusive behavior of the particle near z_{cut} is dominant. Larson and Lightfoot present two approaches for calculating the escape rate of a particle from a Lennard-Jones well in the overdamped regime. The first is in the overdamped *limit*, using the Smoluchowski equation, which is valid for $t_{in} \to 0$, or $\alpha \to \infty$.

$$\tau_{esc} = \tau_0 \left(\frac{\pi\, k_B T}{\varepsilon}\right)^{1/2} \frac{\frac{z_{cut}}{a} - \left(\frac{4\varepsilon}{k_B T}\right)^{1/n} \Gamma\left(1-\frac{1}{n}\right)}{n\, 2^{-1/n}} e^{\varepsilon/k_B T} \qquad \text{Eq. 4}$$

Here the dimensional escape time is τ_{esc}/τ_0, and $n = 6$ is the exponent in the 12-6 LJ potential.

Larson and Lightfoot carried out "exact" calculations confirming these expressions for $z_{cut} = 10\ a$, which is considerably larger than the more practical and frequently used cutoff value of 2.5 a, where the potential is already quite flat. Therefore, we wish to assess the accuracy of the LL theory for a range for cutoff values from 2.5 a to 10 a.

Kramers offers a well-known theory for the escape time of a moderately underdamped to overdamped Brownian particle from a 1-D potential well with upward curved harmonic shape at the bottom and downward harmonic at the top, as shown in Fig 1A. The predicted result depends on the curvatures of the potential at both bottom and top. Near the bottom of the well at $z = z_{min}$, the harmonic is defined by:[7]

$$U(z) = -\varepsilon + \tfrac{1}{2} k (z - z_{min})^2 \ = -\varepsilon + \tfrac{1}{2} m\Omega^2 (z - z_{min})^2, \qquad \text{Eq. 5}$$

where ε is the well depth, and k is a "spring" constant defining the curvature at the bottom of the well. For a particle of mass m, in the above equation we express the constant, k, in terms of a characteristic oscillation frequency Ω as $k = m\Omega^2$, where Ω is the frequency of oscillation of the particle in the well in the underdamped limit where friction is negligible. Similarly, near the top of the well at $z = z_{cut}$, we write

$$U(z) = -\frac{1}{2}k'(z - z_{cut})^2 = -\frac{1}{2}m\ \ ^2(z - z_{cut})^2 \quad \text{Eq. 6}$$

where k' is the magnitude of the curvature around z_{cut}. Expressed in terms of these characteristic frequencies, Kramers' expression for the escape time is

$$\tau_{esc} = \frac{2\pi}{\Omega}\frac{1}{\left[\sqrt{1+\frac{1}{4\omega^2\ t_{in}{}^2}}-\frac{1}{2\omega\ t_{in}}\right]}e^{\varepsilon/k_BT} \quad \text{Eq. 7}$$

For $\frac{1}{2\omega} \gg t_{in}$, which is the overdamped limit, Eq. 7 can be approximated as:

$$\tau_{esc} = \frac{2\pi}{\Omega\omega}\frac{1}{t_{in}}e^{\varepsilon/kT} = \frac{2\pi}{\sqrt{k\prime k}}\zeta e^{\varepsilon/k_BT} \quad \text{Eq. 8}$$

Eq. 8 is widely known and used in the overdamped regime, where the escape time depends only on the bead drag coefficient, ζ, and not on the bead mass.

To attempt to apply Eq. 7 to a potential such as the LJ potential that does not have a negative (downward) curvature at the point of escape, we can artificially create such a region by adding to the original potential a mirror reflection of the Lennard-Jones potential around z_{cut} so that we may define z_{cut} as a local maximum, as shown in Fig. 1C:[9]

$$U_{LJ,m}(z) = 4\varepsilon\left[\left(\frac{\sigma}{z}\right)^{12} - \left(\frac{\sigma}{z}\right)^{6} + \left(\frac{\sigma}{2\ z_{cut} - z}\right)^{12} - \left(\frac{\sigma}{2\ z_{cut} - z}\right)^{6}\right] \quad \text{Eq. 9}$$

We then can use a Taylor expansion to approximate $U_{LJ,m}(z)$ around z_{min} as

$$U_{LJ,m}(z) \cong -\varepsilon + \frac{1}{2}57.15\ \varepsilon\left(\frac{z - z_{min}}{a}\right)^2 \quad \text{Eq. 10}$$

so long as $\left(\frac{z_{min}}{z_{cut}}\right)^7 \ll 1$. Expanding $U_{LJ,m}(z)$ around z_{cut} gives

$$U_{LJ,m}(z) \cong 2 \times 4\varepsilon\left[\left(\frac{\sigma}{z_{cut}}\right)^{12} - \left(\frac{\sigma}{z_{cut}}\right)^{6}\right] + \frac{1}{2} \times 2 \times 4\varepsilon\left[\frac{156\sigma^{12}}{z_{cut}^{14}} - \frac{42\sigma^{6}}{z_{cut}^{8}}\right](z - z_{cut})^2 \quad \text{Eq. 11}$$

The first term amounts to approximately -0.033ε at $z_{cut} = 2.5\sigma$ and decreases for larger z_{cut} values, and thus can be neglected. Thus, only the quadratic term required by Kramers' theory remains. Therefore, the mirrored LJ potential is approximated near z_{cut} as:

$$U_{LJ,m}(z) \cong \frac{1}{2} 8\varepsilon\left[\frac{156a^{12}}{z_{cut}^{14}} - \frac{42a^{6}}{z_{cut}^{8}}\right](z - z_{cut})^2 \quad \text{Eq. 12}$$

Comparing Eq. 5 with Eq. 10 and Eq. 6 with Eq. 12, we find that for the mirrored Lennard-Jones potential:

$$m\Omega^2 = k = 57.15\frac{\varepsilon}{a^2} \quad \text{Eq. 13}$$

$$m\ ^2 = k' = -8\varepsilon\left[\frac{156\sigma^{12}}{z_{cut}^{14}} - \frac{42\sigma^{6}}{z_{cut}^{8}}\right] \quad \text{Eq. 14}$$

where for $z_{cut} = 2.5\ a, m\ ^2 = 0.22\varepsilon$.

2. Underdamped particle

We now will consider the case of an underdamped particle escaping a Lennard-Jones potential well. Kramers' presented a solution for a particle in the underdamped *limit*, which assumes that the rate limiting step is energy uptake from the heat bath:

$$\tau_{esc} = \frac{2\pi}{\Omega}\frac{t_{in}}{S_1}\ e^{\varepsilon/k_B T} \quad \text{Eq. 15}$$

Here S_1 is the "action" per oscillation cycle of the particle, defined as

$$S_1 = 2\int_{1a}^{z_{cut}} \sqrt{[-2mU_{LJ}(z)]}dz \quad \text{Eq. 16}$$

We obtain S_1 by numerical integration of Eq. 16 using N-point quadrature with a spacing of $h = 0.025a$, thus taking the entire shape of the potential-well into account. Eq. 15 can be used to calculate the escape time for given values of $\{t_{in}, m$ and $\varepsilon\}$ using relationships established above (Eqs. 9-11 and 13-14).

The prediction of Eq. 15 is shown in Fig. 2 by the dot-dashed lines for small values of α, and Eq. 7 (which converges to Eq. 8 at high α) is shown by solid lines for large values of α. Mel'nikov and Meshkov (MM) proposed a solution to Kramers problem for all damping regimes, which spans Kramers' two limits (although does not account for the flatness of the LJ potential near the point of escape) and is shown by the dotted lines in Fig. 2A. The MM result, given by Eq. 17, is a more generalized form that encompasses Kramers' Eqs. 7, 8, and 15, and includes the prefactor $A(\Delta)$, which accounts for the coupling of the particle to the heat bath.[8]

$$\tau_{esc} = \frac{2\pi}{\Omega} \frac{1}{\left[\sqrt{1+\frac{1}{4\omega^2 t_{in}^2}} - \frac{1}{2\omega t_{in}}\right]} \frac{1}{A(\Delta)} e^{\varepsilon/k_B T} \qquad \text{Eq. 17}$$

$$\text{where } \Delta = \frac{S_1}{t_{in}\, k_B T}, \qquad \text{Eq. 18}$$

The function $A(\Delta)$ covering all damping regimes is given by:

$$A(\Delta) = \exp\left[-\sum_{n=1}^{\infty} n^{-1} erfc\left[\frac{\sqrt{n\Delta}}{2}\right]\right] \qquad \text{Eq. 19}$$

Where the sum in Eq. 19 converges within $n = 200$ for all the cases studied in this work.

This result derived by Mel'nikov and Meshkov (MM) was originally presented as a solution for a potential with harmonic bottom and harmonic top for all damping regimes. However, it can be seen that both the MM and Kramers' solutions fail in the high-α regime, since the harmonic assumption is a poor approximation for the shape of a LJ well near z_{cut}. Thus, we will see that a complete solution to the escape problem for an LJ potential over all friction regimes requires splicing a low- α solution with the LL solution at high α.

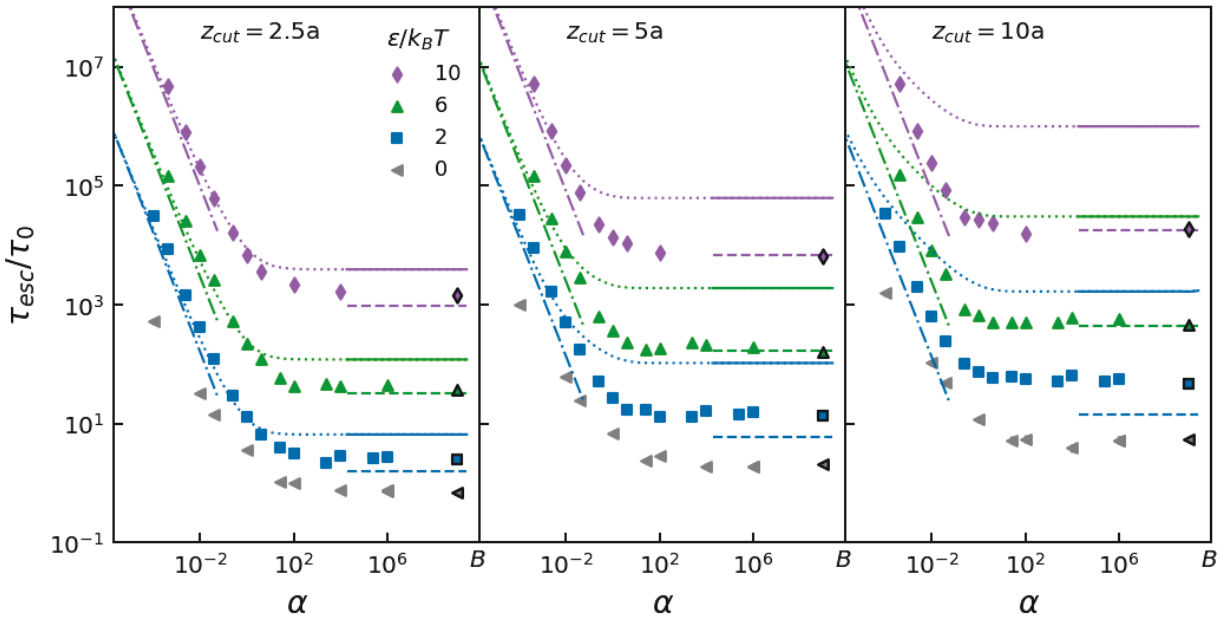

Fig. 2: Symbols represent simulation results for escape of a particle from the LJ potential given in Eq. 3 using HOOMD-blue's Langevin integrator and are the same in each sub-figure. Symbols outlined in black on the far right of each sub-figure are from simulations using HOOMD-blue's Brownian integrator (denoted on the x axis by B). **A)** Dot-dashed lines represent Kramers' theory for an underdamped particle (Eq. 15), solid lines represent Kramers' theory for an overdamped particle (Eq. 7), and the dotted lines represent Mel'nikov-Meshkov theory for all damping regimes (Eq. 17). Dashed lines represent the high friction limit of Larson and Lightfoot (Eq. 4). Line and symbol color designates a given value of ε/k_BT, shown in the legend. There are no lines corresponding to free diffusion, for which ε/k_BT= 0, for which simulation results are denoted by grey symbols.

3. Scaling behavior and solution for all damping regimes

From the LL (Eq. 4), Kramers (Eq. 7 and 8), and MM (Eq. 17) solutions, we can determine scaling laws for the dimensionless escape time τ_{esc}/τ_0 in the overdamped and underdamped limits. In both limits, the dimensionless escape time is proportional to $\exp(\varepsilon/kT)$, with a prefactor of order unity in the overdamped limit.

In the underdamped limit ($\alpha \to 0$, or $t_n \to \infty$), the escape time τ_{esc} from Kramers "general" theory, Eq. 7, and from LL's theory for the underdamped case, approach the scaling of the activated complex theory (ACT)[9], wherein the prefactor is proportional to the inverse of the oscillation frequency Ω in the potential well, and therefore scales as $a\sqrt{m/\varepsilon}$, which is *independent of the friction coefficient* ζ . The normalized escape time τ_{esc}/τ_0, recalling that $\tau_0 \equiv \frac{\zeta a^2}{k_BT}$, therefore has

a prefactor that scales as $\left(a\sqrt{\frac{m}{\varepsilon}}\right)/\frac{\zeta a^2}{k_BT} = \sqrt{k_BT/\varepsilon}\alpha^{-1/2}$. It thus scales as the inverse square root of α. As discussed above, however, this result fails in the limit of $\alpha \to 0$, because of lack of equilibrium with the heat bath, which requires the presence of friction because of the fluctuation-dissipation theorem. Reducing friction allows one to approach the regime in which ACT is valid, but one cannot reach this theory at asymptotically small α, because equilibration with the heat bath is lost as $\alpha \to 0$. Kramers therefore provided a separate equation for this limit, whose results are given by the dot-dashed line in Fig. 2, but only the MM theory bridges to this result continuously as $\alpha \to 0$.

The MM theory in the $\alpha \to 0$ limit therefore differs from Kramers "general" theory, Eq. 7, by the additional factor of $A(\Delta)$ (Eq.19) in the denominator, where Δ scales as $a\sqrt{\frac{\varepsilon}{m}}\frac{\zeta}{k_BT}$. Thus, the low-$\alpha$ behavior of the MM solution depends on the scaling of $A(\Delta)$ with Δ at low Δ. Mel'nikov and Meshkov report that $A(\Delta) \quad \Delta - 0.82\Delta^{/2}$ at low α, which we can approximate by $A(\Delta) \quad \Delta$ in the asymptotic limit. We thus find that $\frac{\tau_e\ c}{\tau} \quad \left(a\sqrt{\frac{m}{\varepsilon}}\right)/\left(\frac{\zeta a^2}{k_BT}\Delta\right)\exp\left(\frac{\varepsilon}{k_BT}\right)$, which is $\frac{\tau_e\ c}{\tau}$ $\sim(\frac{k_BT}{\varepsilon})\alpha^{-1}\exp(\frac{\varepsilon}{k_BT})$, where there is scaling of dimensionless escape time with α^{-1}, rather than $\alpha^{-1/2}$. This scaling of α^{-1} at low α is consistent with the observed scaling of the MM theory, the Kramers $\alpha \to 0$ limit (Eq. 15), and the Langevin simulations, as seen in Fig. 2. In dimensional terms, in the underdamped limit, $\tau_{esc} \quad \frac{m}{\zeta}\frac{k_BT}{\varepsilon}\exp\left(\frac{\varepsilon}{k_BT}\right)$, where $\frac{m}{\zeta}$ is the inertial time, and the escape time is inversely proportional to the drag coefficient ζ, while in the overdamped limit $,\tau_{esc} \quad \frac{\zeta a^2}{k_BT}\exp(\varepsilon/kT)$, it is proportional to ζ. In between these, in the ACT pseudo-limit, $\tau_{esc} \quad a\sqrt{m/\varepsilon}\exp\left(\frac{\varepsilon}{k_BT}\right)$, which is independent of ζ.

When the escape time is scaled by the frictional time τ_0, the prefactor of $\exp(\varepsilon/k_BT)$ from the LL equation for the overdamped limit (Eq. 4) is independent of α and that from Kramers' equation for an underdamped particle (Eq. 15) in the limit of small alpha is proportional to α^{-1}. Combining these two regimes into a cross-over formula gives (Eq. 22). The prefactor of $\exp(\varepsilon/k_BT)$ in the overdamped limit, $B_{LL}(\varepsilon/k_BT)$, is constant with respect to α, while the prefactor of

$\alpha^{-1}\exp(\varepsilon/k_BT)$ in the underdamped limit, $B\ (\varepsilon/k_BT)$ is a constant with respect to α from Kramers' Eq. 15. Thus,

$$B_{LL}(\varepsilon/k_BT) = \left(\frac{\pi\, k_BT}{\varepsilon}\right)^{1/2} \frac{\frac{z_{cut}}{a} - \left(\frac{4\varepsilon}{k_BT}\right)^{1/n}\Gamma\left(1-\frac{1}{n}\right)}{n\, 2^{-1/n}} \quad \text{Eq. 20}$$

$$B\ (\varepsilon/k_BT) = \frac{\pi\, a\, k_BT}{\sqrt{2}\sqrt{57.15\,\varepsilon}} \frac{1}{\int_{1a}^{z_{cut}} \sqrt{[-\ (z)]}dz} \quad \text{Eq. 21}$$

$$\tau_{esc}/\tau_0 = \left(B_{LL}(\varepsilon/k_BT) + \frac{B_K(\varepsilon/k_BT)}{\alpha}\right) e^{\varepsilon/k_BT} \quad \text{Eq. 22}$$

The prediction of Eq. 22 is shown as dashed lines in Fig. 3A. This result reaches the correct asymptotes for high and very low α , but does not capture the transition between the two accurately and leaves out the ACT pseudo limit which influences the behavior at intermediate α. The reason for this deviation in the region of moderately small α is that while the assumption that $A(\Delta) = \Delta$ holds true in the underdamped *limit*, this limit is not reached until α is very small, as shown in Fig. 3B. For a more accurate solution, which also captures the ACT pseudo-limit, we can keep the exact form of the $A(\Delta)$ correction factor in the denominator, thus using the prefactor from Mel'nikov and Meshkov's approach in Eq. 10. In this case, the prefactor of $\exp(\varepsilon/k_BT)$, which is $B\quad(\alpha, \varepsilon/k_BT)$, is not independent of α , but still scales as α^{-1} in the limit of very small α. That is,

$$B\quad(\alpha,\ \varepsilon/k_BT) = \frac{2\pi}{\Omega}\ \frac{1}{A(\Delta)\ \tau} \quad \text{Eq. 23}$$

The form of the general equation is then

$$\frac{\tau_{e\ c}}{\tau} = \left(B_{LL}(\varepsilon/k_BT) + B\quad(\alpha, \varepsilon/k_BT)\right)e^{\varepsilon/k_BT} \quad \text{Eq. 24}$$

whose predictions, shown by the solid lines in Fig. 3A, are in much better agreement with the simulation data than are those from Eq. 22, given by the dashed lines in Fig. 3A. Eq. 24 is therefore

the most complete solution for this case of escape from a Lennard-Jones potential for arbitrary damping.

This solution also allows us to distinguish within the underdamped regime the conditions for which the rate of energy uptake from the heat bath is limiting (i.e., "very small" α) from those for which it is not limiting. To do so, we plot in Fig. 3C the prefactor of Eq. 24, namely $B_{LL}(\varepsilon/k_BT) + B\quad(\alpha, \varepsilon/k_BT)$ against α for various values of ε/k_BT, noting that a clear regime in which the prefactor scales as $\alpha^{-1/2}$ appears only for very high ε/k_BT, around 10,000 or higher. For smaller ε/k_BT, the rate of energy uptake from the heat bath is not limiting only when α is high enough to be out of the underdamped limit, and on the way towards overdamping. Only for very high $\varepsilon/k_BT \geq$ 10,000, there is a clear $\alpha^{-1/2}$ underdamped scaling regime between "very small" α (with scaling α^{-1}) and the overdamped regime. The huge value of ε/k_BT required to obtain this regime, and the exponential dependence of escape time on ε/k_BT, imply that this intermediate regime, described by the "Activated Complex Theory" (ACT), for which the escape time is independent of the friction coefficient, is therefore essentially always a rough approximation.

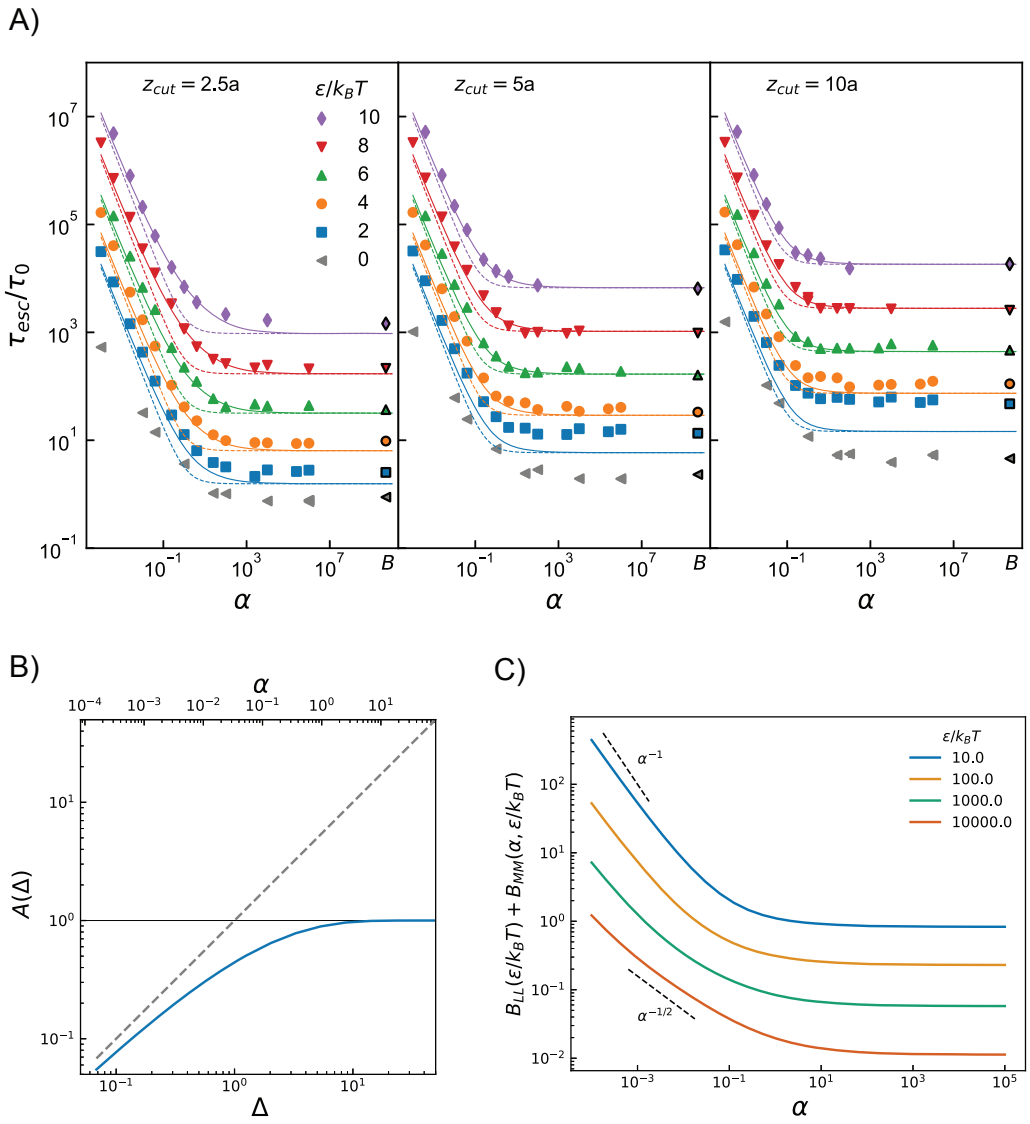

Fig. 3: A) All symbols are the same as in Fig. 2. Dashed lines represent Eq. 22, using $B\ (\varepsilon/k_BT)$, and solid lines represent the theory presented in Eq. 24, using $B\ \ (\alpha, \varepsilon/k_BT)$. B) Blue line: $A(\Delta)$ as given in Eq. 19 and grey dashed line: $A(\Delta) = \Delta$, both for $\varepsilon = 8\ kT$, $z_{cut} = 2.5\ a$. C) Prefactor from Eq. 24 for where $z_{cut} = 10\ a$. Black dotted lines indicate scaling for α^{-1} and $\alpha^{-1/2}$, as indicated on the plot.

Now that we've shown the ranges of validity of each of the important theories, we consider a specific problem where attainment of the overdamped limit is important and where ignorance of the above information led to an error in a paper published earlier by our group.

Example Problem: Colloid-Polymer Mixtures

Here we demonstrate the relevance of these considerations by noting the need for a correction to Wang and Larson's recent report of Langevin dynamics simulations of the multiple relaxation modes displayed in an aqueous suspension of colloidal particles of radii R=10 a or R=25 a and telechelic polymers.[10] The telechelic polymers were modeled by dumbbells, with each bead able to bind to the surface of a colloid, where binding was controlled by an attractive potential well bounding the surface of each colloid. This potential well allowed the formation of polymer *loops* on a single colloid particle when both beads of a dumbbell were bound to the same colloid, or of *bridges* between neighboring particles, when the two beads were bound to different colloids.[10] The fastest relaxation times in the simulations involved diffusion of a polymer loops across the surface of the particle, while a slower relaxation process was the breakage of a bridge by escape of one of the beads from the colloid surface. The colloid radius was large enough that the diffusion of the loop over the surface of the particle was able to reach the overdamped regime over the time required for chain relaxation, as demonstrated by changing the dumbbell bead friction. Wang and Larson naively assumed that all slower relaxation processes would then also be overdamped using the same Langevin simulator, including the relaxation involving breakage of the bridge.

However, as is evident from our simulations and our above discussion, the slow escape of the bead from a narrow potential binding a dumbbell bead to the colloid can be underdamped even when a faster free diffusion of the same particle is overdamped. Fig. 4 shows a correction to Wang and Larson's Fig. 5, including the original data from Wang and Larson (blue symbols) along with our replication of the study using HOOMD-blue's Langevin and Brownian integrators (orange and green square symbols, respectively). Our simulations here thus show that the particles' escape from the L-J was not overdamped in Wang and Larson's paper, and as a result, the bridge breakage process proved to be outside of the overdamped regime, despite the much faster loop diffusion process being overdamped.

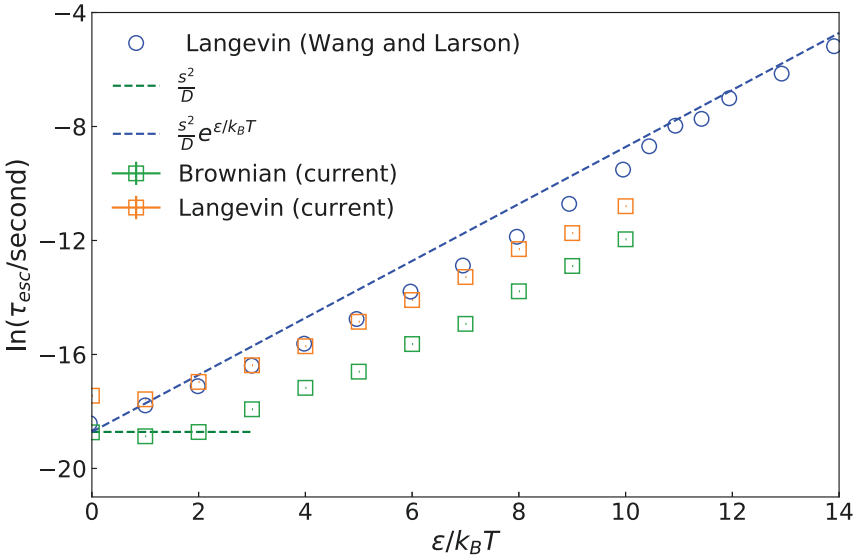

Fig. 4: Wang and Larson's times of escape, τ_{esc}, of a particle of drag coefficient ζ and diffusivity $D = k_BT/\zeta$ from a potential well of depth ε calculated from Langevin dynamics using LAMMPS (blue circles) compared with escape times from Brownian dynamics (green squares) and Langevin dynamics (orange squares) using HOOMD-blue. Simulations are averages of escape times over 100 stickers, initialized on the surface of a colloidal particle with diameter $D_{co\ \ oid} = 20\ a$, as described in the original paper. Predictions from Pham *et al*[12] with and without a potential (blue and green dashed lines) are included for $s = (r_c - r_m) = 1.\ 8\ a$. Parameters used in these simulations: time step $\Delta t = 0.001\tau_R$, mass $m = 1.0\ m_0$ and friction coefficient $\zeta = 1.0\ m_0\ \ \tau_R$.

As a result, as shown in Fig. 5, the predicted results from Wang and Larson for the relaxation modulus of a network of colloids bridged by dumbbells is sensitive to the dimensionless inertial time τ_{in}/τ_R down to values of around 10^{-2} rather than reaching convergence at unity, as was naively assumed by Wang and Larson. The slow bridge breakage was not in the overdamped regime even while the fast loop diffusion was overdamped because the width of the potential well binding the bead was less than the distance of free diffusion required for loops relaxation. This can be anticipated by the results in Fig. 3, by noting that the transition from underdamped to overdamped behavior is only completed when α reaches approximately 10^2-10^3, regardless of the well depth, or even the presence of a potential, as shown by the grey symbols for $\varepsilon = 0$. For free diffusion over the surface of the particle, the relevant length scale is comparable to the colloid radius, and the length scale a in the expression $\alpha \equiv \frac{\zeta^2\, a^2}{m\, k_BT}$ shown be taken as the colloid radius R, while for escape from the potential well, a is the well width, which was an order of magnitude or

more smaller than R. Thus, the relevant value of α was high enough to attain the overdamped limit for free diffusion, but too low to attain this limit for the much slower escape from the potential well. Failing to consider the appropriate condition for attaining the overdamped regime when a conservative force was present, Wang and Larson unwittingly presented results that were significantly affected by inertia.

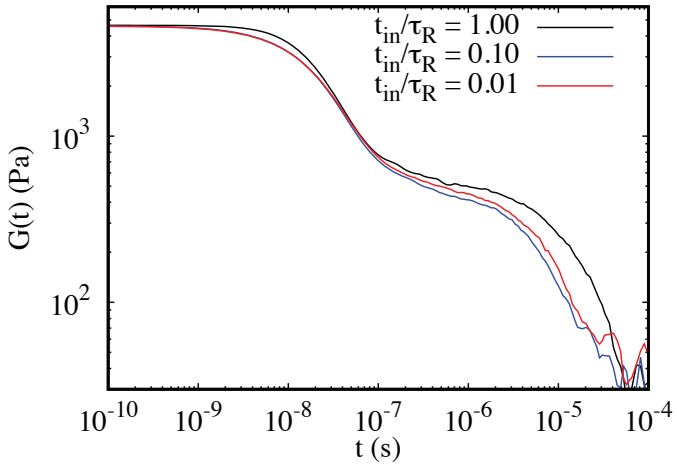

Fig. 5: Effect of dimensionless inertial time t_{in} on relaxation modulus computed by Langevin simulations, for the problem described in Fig. 4 of Wang and Larson. In the Wang-Larson paper, $\frac{t_{in}}{\tau_R}$ was taken to be 1.0, which is outside of the overdamped limit, as shown by its effect on the result.

Finally, we note that the combined formula for the escape time given above is valuable not only for determining conditions needed for reaching the overdamped regime in Langevin simulations, but also gives a good estimate of the escape time in situations where a good estimate of the escape time is needed. An example is the case of mesoscale population-balance simulations in which the polymers are included only implicitly and rates of breakage and formation of bridges must be given by explicit formulas.[13]

Conclusion

In Langevin simulations of systems with multiple relaxation processes, especially those involving escape from potential wells, attainment of the overdamped regime requires careful attention to the dimensionless damping coefficient, α. We assessed the validity of theories from Kramers, Mel'nikov and Meshkov (MM), and Larson and Lightfoot (LL) for all damping regimes by

comparison to Langevin dynamics simulations of a particle escaping from a 12-6 Lennard-Jones potential. We demonstrate that the standard Kramers theory is not accurate for a Lennard-Jones potential in the underdamped regime because it does not account for the coupling of the particle to the heat bath, and in the overdamped regime because it does not apply to a potential that becomes flat near the escape condition, as is the case for the LJ potential. Because MM theory is accurate in the underdamped regime for an arbitrary potential, and LL theory is accurate in the overdamped regime for the LJ potential, we determine prefactors from each of these approaches that allow presentation of a general equation for arbitrary damping for escape from an LJ potential well. This general theory also shows that the validity of the Activated Complex Theory (ACT) is limited to extraordinarily high values of the dimensionless well depth.

Acknowledgement

This work was supported in part by the National Science Foundation (NSF) under Grant. Any opinions, findings, and conclusions or recommendations expressed in this material are those of the authors and do not necessarily reflect the views of the NSF. E.M. acknowledges the funding support from United States—India Educational Foundation (USIEF) via Fulbright-Nehru Academic and Professional Excellence (FNAPE) fellowship 2019–2020.

References

1. P. Howard, M., Nikoubashman, A. & Z. Panagiotopoulos, A. Stratification in Drying Polymer–Polymer and Colloid–Polymer Mixtures. *Langmuir* **33**, 11390–11398 (2017).
2. Omar, A. K. & Wang, Z.-G. Shear-Induced Heterogeneity in Associating Polymer Gels: Role of Network Structure and Dilatancy. doi:10.1103/PhysRevLett.119.117801
3. Wu, H. *et al.* Spatiotemporal Formation and Growth Kinetics of Polyelectrolyte Complex Micelles with Millisecond Resolution. *ACS Macro Lett.* **9**, 1674–1680 (2020).
4. Ge, T., Rubinstein, M. & S. Grest, G. Effects of Tethered Polymers on Dynamics of Nanoparticles in Unentangled Polymer Melts. *Macromolecules* **0**, (2020).
5. Anderson, J. A., Glaser, J. & Glotzer, S. C. HOOMD-blue: A Python package for high-performance molecular dynamics and hard particle Monte Carlo simulations. *Comput. Mater. Sci.* **173**, 109363 (2020).
6. Plimpton, S. Fast Parallel Algorithms for Short-Range Molecular Dynamics. *J. Comput. Phys.* **117**, 1–42 (1997).
7. Kramers, H. A. Brownian motion in a field of force and the diffusion model of chemical reactions. *Physica* **7**, 284–304 (1940).
8. Mel'nikov, V. I. & Meshkov, S. V. Theory of activated rate processes: Exact solution of the Kramers problem. *J. Chem. Phys.* **85**, 1018–1027 (1986).
9. Larson, R. S. & Lightfoot, E. J. Thermally activated escape from a Lennard-Jones potential well. *Phys. A Stat. Mech. its Appl.* **149**, 296–312 (1988).
10. Wang, S. & Larson, R. G. Multiple relaxation modes in suspensions of colloidal particles bridged by telechelic polymers. *J. Rheol. (N. Y. N. Y).* **62**, 371 (2018).
11. Pollak, E. & Ankerhold, J. Improvements to Kramers turnover theory. *J. Chem. Phys.* **138**, 164116 (2013).
12. Pham, Q. T., Russel, W. B. & Lau, W. Rheology of telechelic associative polymers in aqueous solutions. *Cit. J. Rheol.* **42**, 979 (1998).
13. Hajizadeh, E., Yu, S., Wang, S. & Larson, R. G. A novel hybrid population balance—Brownian dynamics method for simulating the dynamics of polymer-bridged colloidal latex particle suspensions. *J. Rheol. (N. Y. N. Y).* **62**, (2018).